Radiation Physics and Chemistry 81 (2012) 728–734

Contents lists available at SciVerse ScienceDirect

Radiation Physics and Chemistry

journal homepage: www.elsevier.com/locate/radphyschem

Nature of bonding in $CaTiO_3$ and $SrTiO_3$: A Compton scattering study

K.C. Bhamu [a], Alpa Dashora [a], Gunjan Arora [b], B.L. Ahuja [a,*]

[a] Department of Physics, M.L. Sukhadia University, Udaipur 313001, Rajasthan, India
[b] Department of Physics, Techno India NJR Institute of Technology, Udaipur 313002, Rajasthan, India

ARTICLE INFO

Article history:
Received 30 December 2011
Accepted 19 April 2012
Available online 27 April 2012

Keywords:
X-ray scattering
Band structure calculations
Density functional theory
Titanates

ABSTRACT

Compton profile measurements for $CaTiO_3$ and $SrTiO_3$ perovskite compounds have been undertaken using 20 Ci ^{137}Cs Compton spectrometer. To understand the nature of bonding in both the compounds, we have analyzed the Compton line shape in terms of equal-valence-electron-density profiles. Electron momentum densities, energy bands and density of states computed using linear combination of the atomic orbitals method (within the framework of density functional theory) are analyzed using the experimental Compton line shapes. It is seen that the recently developed second order generalized gradient approximation gives a better description of momentum densities than the local density approximation. Moreover, bonding in both the ceramic compounds has also been discussed in terms of Mulliken's population analysis.

1. Introduction

$CaTiO_3$ and $SrTiO_3$ are perovskite ceramic materials with tremendous scientific and technological applications (Orhan et al., 2004; Ali and Yashima, 2005). $CaTiO_3$ is widely used in electronic ceramic materials, immobilizing high level radioactive waste and microwave devices, etc. (Ringwood et al., 1988; Newnham and Ruschau, 1991; Wang et al., 2001; Hui-Ping et al., 2007). $SrTiO_3$ is useful in optoelectronics and microelectronics components such as micro-capacitors, ultrathin gate chips and optical switches. Because of its high dielectric constant, $SrTiO_3$ is an attractive material for tunneling semiconductor valves and magnetic tunnel junctions for spintronics applications (Mo and Ching, 1999; Bacq et al., 2006).

Regarding earlier important studies, few investigations on the structural, electronic and optical properties of these perovskites are available in literature. Fabricius et al. (1997) have compared energy bands and density of states (DOS) of $SrTiO_3$ and $SrHfO_3$ using local density approximation (LDA) within full potential linearized augmented plane wave (FP-LAPW) scheme. Saha et al. (2000) have made a detailed study on electronic and optical properties of $CaTiO_3$ using tight-binding linear muffin-tin orbitals (TB-LMTO) method. A first-principle study on nature of ferroelectricity of $CaTiO_3$ has been reported by Wang et al. (2001). Yuan-Xu et al. (2002) have studied the ferroelectric behavior of $CaTiO_3$ and $SrTiO_3$ using the FP-LAPW method. Electronic structure and optical properties in the core level spectra of $SrTiO_3$ have been computed by Cai et al. (2004) using first-principle with scissor approximation. Ali and Yashima (2005) have determined the space group and the crystal structure of $CaTiO_3$ in the temperature range 296–1720 K. Using FP-LAPW method, Hui-Ping et al. (2007) have studied the optical properties (absorption coefficients, reflectivity, dielectric behavior, etc.) of $CaTiO_3$. Zhen-Ye et al. (2007) have investigated polarization behavior of different types of super lattices. Due to lack of data on momentum density and also a comparative study on nature of bonding of both the isoelectronic perovskites ($CaTiO_3$ and $SrTiO_3$), a systematic study of Compton profiles is highly required.

It is worth mentioning that the Compton profile (CP) represents a one-dimensional projection of electron momentum density $\rho(\mathbf{p})$ along the scattering vector (Cooper, 1985; Ahuja, 2010). Mathematically, the CP, $J(p_z)$ is defined as

$$J(p_z) = \int_{p_x}\int_{p_y} \rho(\mathbf{p}) dp_x\, dp_y \propto \frac{d^2\sigma}{d\Omega\, d\omega_2}, \quad (1)$$

where p_z is the component of electron momentum along the z-axis (parallel to the scattering vector). $d\Omega$ is the solid angle element of the scattered beam. An electron with momentum p_z shifts the energy of photon from ω_1 (incident) to ω_2 (scattered at an angle θ). A conversion of energy into momentum p_z is given by the relation:

$$p_z = \frac{mc\{\omega_2 - \omega_1 + \omega_1\omega_2(1-\cos\theta)/mc^2\}}{(\omega_1^2 + \omega_2^2 - 2\omega_1\omega_2\cos\theta)^{1/2}}. \quad (2)$$

Here m and c are the rest mass of electron and velocity of light, respectively. One atomic unit (a.u.) of momentum is equal to 1.9929×10^{-24} kg m s^{-1}.

The purpose of the present CP studies is multifold, namely (a) to compare the Compton profiles of $CaTiO_3$ and $SrTiO_3$ using

* Corresponding author. Tel.: +91 94143 17048; fax: +91 294 2411950.
E-mail address: blahuja@yahoo.com (B.L. Ahuja).

0969-806X/$ - see front matter © 2012 Elsevier Ltd. All rights reserved.
http://dx.doi.org/10.1016/j.radphyschem.2012.04.010

20 Ci ^{137}Cs Compton spectrometer in terms of equal-valence-electron-density (b) to compute theoretical profiles, energy bands, density of states and Mulliken's population of both the perovskites using density functional theory and (c) to compare theoretical and experimental CPs and to analyze the Compton profiles in terms of energy bands and Mulliken's population.

2. Experiment

The CP measurements were carried out on high purity ($\geq$99.9) polycrystalline $CaTiO_3$ and $SrTiO_3$ (procured from Alfa–Aesar) using a high energy 20 Ci ^{137}Cs Compton spectrometer. The resolution (Gaussian, full width at half maximum) of the spectrometer was 0.34 a.u. More information on the experimental set-up can be found elsewhere (Ahuja et al., 2006). In individual measurements, the high-energy γ-rays of 661.65 keV were scattered at an angle of $160\pm0.6^{\circ}$ by both the samples. The scattered photons were recorded by a high purity Ge detector (Canberra, Model GL0510P) and associated electronics. Other experimental parameters like, sample thickness, diameter, bulk densities and integrated counts under Compton peak are collated in Table 1. To achieve true CPs, raw data were subsequently corrected for background, sample absorption, instrumental resolution (limited to stripping off the low-energy tail), detector efficiency and Compton cross-section (Timms, 1989). Correction for multiple (up to triple) scattering was also applied using the Monte Carlo simulation (Felsteiner et al., 1974). To simulate the multiple scattering contribution, we have considered the history of one million photons for both the compounds. The effect of multiple scattering is also given in Table 1. In Fig. 1, we have plotted the spectral distribution of single, double and triple scattering with the incident photon energy for both the compounds. As expected, the single scattering contribution is higher in comparison to double and triple scattering. In Fig. 1(a), $SrTiO_3$ gives an overall broadened spectra of single scattered photons in comparison to $CaTiO_3$, which may be due to 3d electrons of Sr in $SrTiO_3$. It is also observed that most of the features on the double (Fig. 1b) and triple (Fig. 1c) scattering distribution curves are almost similar for both the iso-electronic compounds. Finally, the corrected experimental CPs were normalized on the corresponding area of free atom CPs (Biggs et al., 1975) within the momentum range 0–7 a.u. (Table 1).

3. Theory

Theoretical CPs, energy bands, DOS and Mulliken's population analysis for $CaTiO_3$ and $SrTiO_3$ were computed using linear combination of atomic orbitals (LCAO) scheme as embodied in CRYSTAL09 package (Dovesi et al., 2009). In this method, the crystalline orbitals, $\psi_i(\mathbf{r};\mathbf{k})$, are expanded as linear combination of Bloch functions, $\varphi_\mu(\mathbf{r};\mathbf{k})$, defined in terms of local orbitals, $\chi_\mu(\mathbf{r}-A_\mu-\mathbf{g})$, as

$$\psi_i(\mathbf{r};\mathbf{k})=\sum_\mu c_{\mu,i}\phi_\mu(\mathbf{r};\mathbf{k}) \text{ and } \phi_\mu(\mathbf{r};\mathbf{k})=\sum_{\mathbf{g}}\chi_\mu(\mathbf{r}-A_\mu-\mathbf{g})e^{i\mathbf{k}\cdot\mathbf{g}}. \quad (3)$$

Here A_μ denotes the coordinates of the nucleus in the zero reference cell on which ϕ_μ is centered, and the $\sum_{\mathbf{g}}$ is extended to the set of all lattice vectors $\mathbf{g}$. CRYSTAL09 code uses the Gaussian type orbitals (GTO) to expand the $\chi_\mu(\mathbf{r}-A_\mu-\mathbf{g})$ as

$$\chi_\mu(\mathbf{r}-A_\mu-\mathbf{g})=\sum_j^{n_G} C_j G(\varsigma_j,\mathbf{r}-A_\mu-\mathbf{g}) \quad (4)$$

The above relation represents contraction of the n_G primitive Gaussians $G(\varsigma_j,\mathbf{r}-A_\mu-\mathbf{g})$ with predefined exponents ς_j, weighted by the contraction coefficient C_j. Before computing the CP (Eq. (1)), the $\rho(\mathbf{p})$ is deduced using the relation

$$\rho(\mathbf{p})=\frac{1}{V_{BZ}}\sum_j\int_{BZ}dk|\psi_i(\mathbf{p},\mathbf{k})|^2\theta(\varepsilon_F-\varepsilon_j(\mathbf{k})). \quad (5)$$

Here ε_F and ε_j are the Fermi energy and one-electron energy corresponding to $\psi_i(\mathbf{p},\mathbf{k})$ (which is derived from the Fourier transformation of $\psi_i(\mathbf{r},\mathbf{k})$), respectively. θ is the step function and V_{BZ} is the volume of the Brillouin zone (BZ).

The exchange and correlation effects were treated within LDA, generalized gradient approximation (GGA) and the recently developed second order GGA (SO-GGA) of DFT scheme. In the

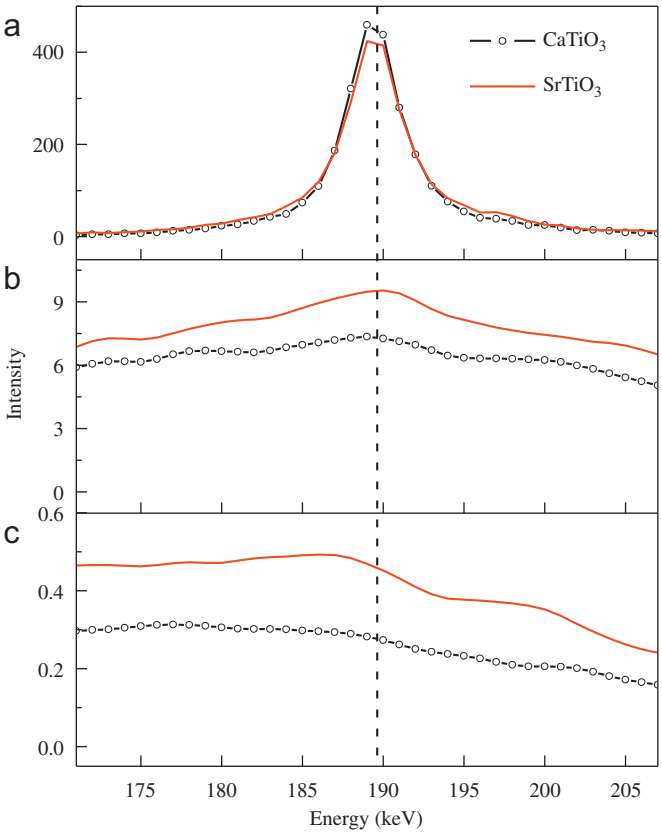

Fig. 1. Spectral distribution of (a) single (b) double and (c) triple scattering for $CaTiO_3$ and $SrTiO_3$ computed using Monte Carlo simulation for one million photons within the energy range of 171–207 keV. The broken line indicates the position of Compton peak (at $p_z=0$ a.u.).

Table 1
Experimental parameters during Compton scattering of 661.65 keV γ-rays from $CaTiO_3$ and $SrTiO_3$ samples and data analysis.

Sample	Sample diameter [thickness] (cm)	Bulk density (gm/cm^3)	Exposure time (h)	Integrated counts	Multiple scattering (-10 to $+10$ a.u.) (%)	Normalization of profile (0 to $+7$ a.u.) (e$^-$)
$CaTiO_3$	2.54 [0.59]	1.87	208	2.40×10^7	10.85	30.69
$SrTiO_3$	2.54 [0.46]	2.73	130	1.54×10^7	11.03	37.52